Filtering a distribution simultaneously in real and Fourier space

Eduardo Anglada and José M. Soler
Departamento de Física de la Materia Condensada, C-III, Universidad Autónoma de Madrid, E-28049 Madrid, Spain
(Received 23 December 2005; published 29 March 2006)

We present a method to filter a distribution so that it is confined within a sphere of given radius r_c and, simultaneously, whose Fourier transform is optimally confined within a sphere of radius k_c. Our procedure may have several applications in the field of electronic structure methods, like the generation of optimized pseudopotentials and localized pseudocore charge distributions. As an example, we describe a particular application within the SIESTA method for density functional calculations, in removing the spurious rippling of the energy surface generated by the integrations in a real-space grid.

DOI: 10.1103/PhysRevB.73.115122 PACS number(s): 71.15.−m, 31.15.Pf

I. INTRODUCTION

It is well known that the mean quadratic widths, in real and Fourier space, Δr^2 and Δk^2, of a distribution in a space of n_D dimensions obey the uncertainty relation $\Delta r \Delta k \geqslant n_D/2$. The equals sign applies to a spherically symmetric Gaussian distribution, which is therefore optimally confined in phase space in the least-squares sense. In many practical cases, however, we are interested in distributions that are strictly confined within a sphere of given radius (i.e., defined to be strictly zero outside that sphere) and, simultaneously, optimally confined within another sphere in Fourier space. This occurs when, to be computationally efficient, we use distributions defined only within a finite sphere and we must limit also their Fourier transforms to a finite number of plane waves. In order to calculate those Fourier components, we frequently must perform a discrete Fourier transform using a finite number of grid points, and we want to avoid as much as possible the resulting aliasing effects.[1] Such a situation occurs, for example, in the efficient computation of Ewald sums, and in the particle-mesh method.[2] Within the field of electronic structure calculations, this problem occurs in the real-space formulation[3] of Kleinman-Bylander pseudopotentials,[4] and of pseudocore charge distributions of ultrasoft pseudopotentials.[5]

In the specific case of the SIESTA density functional method,[6,7] this problem arises in the evaluation, using a real-space grid, of matrix elements involving strictly localized basis orbitals and neutral-atom potentials. Those integrals generate an artificial rippling of the total energy, as a function of the atomic positions relative to the grid points (the so-called eggbox effect), which complicates considerably the relaxation of the geometry and the evaluation of phonon frequencies by finite differences. In other grid-based methods,[8] this problem is generally solved by filtering the atomic pseudopotentials,[9] typically by multiplying them by an *ad hoc* filter function in Fourier space.[1] Here we present a new method for optimal filtering and its application to solve the eggbox problem in SIESTA.

II. OPTIMIZED FILTERING METHOD

We will study only the specific case of three dimensions, but the extension to one or two dimensions is obvious. Consider an initial distribution of the form

$$F(\mathbf{r}) = \begin{cases} F(r)Y_l^m(\hat{\mathbf{r}}), & \text{if } r \leqslant r_c, \\ 0 & \text{otherwise}, \end{cases} \tag{1}$$

where we are using the same symbol F for $F(\mathbf{r})$ and its radial part $F(r)$, since it does not lead to any confusion. $Y_l^m(\hat{\mathbf{r}})$ is a real spherical harmonic. The Fourier transform of $F(\mathbf{r})$ is

$$G(\mathbf{k}) \equiv \frac{i^l}{(2\pi)^{3/2}} \int d\mathbf{r}^3 e^{-i\mathbf{kr}} F(\mathbf{r}) = G(k) Y_l^m(\hat{\mathbf{k}}) \tag{2}$$

where we have introduced the factor i^l to make $G(\mathbf{k})$ real, and

$$G(k) = \frac{4\pi}{(2\pi)^{3/2}} \int_0^{r_c} dr\, r^2 j_l(kr) F(r) \tag{3}$$

where $j_l(x)$ is a spherical Bessel function.

In general $G(k)$ will be nonzero for any value of k. If we want to filter it out for $k > k_c$, the most straightforward procedure is to multiply it by a step function and then to perform the inverse Fourier transform:

$$F(r) \leftarrow \frac{4\pi}{(2\pi)^{3/2}} \int_0^{k_c} dk\, k^2 j_l(kr) G(k). \tag{4}$$

The new $F(r)$ will no longer be strictly zero for $r > r_c$ but we may suppress those components and iterate the procedure. As a result, only the most confined components, in real and reciprocal space, will survive.

To analyze more rigorously the decomposition of $F(r)$ into more and less confined components, let us define $x \equiv r/r_c$, $y \equiv k/k_c$, $f(x) \equiv xF(xr_c)$, $g(y) \equiv yG(yk_c)$, $\kappa \equiv k_c r_c$, and $K(x,y) \equiv \sqrt{2\kappa/\pi}\kappa x y j_l(\kappa x y)$. Then, substituting in Eqs. (3) and (4), one iteration of the filtering procedure is given by

$$f(x) \leftarrow \int_0^1 dx' K^2(x,x') f(x') \tag{5}$$

where

$$K^2(x,x') \equiv \int_0^1 dy\, K(x,y) K(y,x'). \tag{6}$$

If $f(x)$ were already a perfectly confined function in both real and reciprocal space, it would not be affected by the

filtering procedure (5), i.e., it would be an eigenfunction of the filtering kernel K^2 with eigenvalue 1. In practice, the uncertainty principle forbids simultaneous perfect confinement in real and Fourier space, and the filtered $f(x)$ will unavoidably "leak" somewhat outside $x>1$ and its norm within $x\leqslant 1$ will no longer be 1. In fact, if $\phi(x)$ is an eigenfunction of K^2, with norm equal to one within $x\leqslant 1$, its eigenvalue λ^2 gives directly its norm after filtering, since the effect of filtering is just a multiplication by λ^2:

$$\phi(x) \leftarrow \int_0^1 dx' K^2(x,x')\phi(x') = \lambda^2\phi(x). \tag{7}$$

Thus, we may perform an efficient filtering, without the need of iteration, by expanding the original function in terms of the complete basis of eigenfunctions of K^2, keeping only those with eigenvalues sufficiently close to 1. Since it is clear that the eigenfunctions $\phi_i(x)$ of $K(x,y)$, with eigenvalues λ_i, are also eigenfunctions of $K^2(x,x')$, with eigenvalues λ_i^2, we may work with the simpler eigenvalue problem

$$\int_0^1 dy K(x,y)\phi_i(y) = \lambda_i\phi_i(x). \tag{8}$$

Notice that, since $K(x,y)$ is the Fourier-transform kernel, the eigenfunctions $\phi_i(x)$ have the same shape in real and reciprocal space. This is not true in general for the filtered function $f(x)$, which is a combination of eigenfunctions with eigenvalues λ_i close to either $+1$ or -1, which either change sign or not when Fourier transformed.

In order to solve (8), it is convenient to expand $K(x,y)$ and $\phi_i(x)$ in a basis of functions in the interval [0, 1]. The simplest basis is that of powers of x. From the Taylor expansion of $j_l(x)$ at $x=0$ we find $K(x,y)\simeq\Sigma_{n=0}^{N} K_n x^{2n+l+1} y^{2n+l+1}$, where

$$K_n = \sqrt{\frac{2\kappa}{\pi}}\frac{(-1)^n\kappa^{2n+l+1}}{(2n)!!(2n+2l+1)!!}. \tag{9}$$

Then making $\phi_i(x)=\Sigma_{n=0}^{N}\phi_{in}x^{2n+l+1}$, Eq. (8) becomes

$$\sum_{m=0}^{N}\frac{K_n}{2n+2m+2l+3}\phi_{im} = \lambda_i\phi_{in}. \tag{10}$$

In practice, we have found numerically more accurate, stable, and efficient (requiring a lower N) to expand $K(x,x')$ in orthonormal Legendre polynomials[1] $P_n(x)$ in the interval $0\leqslant x\leqslant 1$. Other choices, like Chevyshev polynomials, might be equally suitable. Taking into account the parity $l_p=\mathrm{mod}(l,2)$ of $j_l(x)$:

$$K(x,y) \simeq \sum_{n,m=1}^{N} K_{nm}P_{2n-l_p-1}(x)P_{2m-l_p-1}(y). \tag{11}$$

The kernel coefficients K_{nm} may be calculated by integration in a Gauss-Legendre[1] set of points x_α and weights w_α:

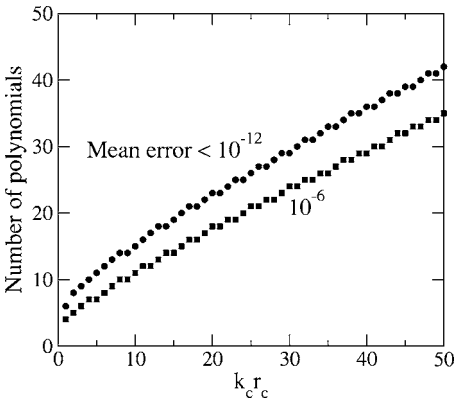

FIG. 1. Number of polynomials required to obtain a root mean square error of the expansion of $xj_0(x)$ in the interval $0<x<k_c r_c$. $j_0(x)$ is a spherical Bessel function with $l=0$.

$$K_{nm} = \int\int_0^1 dx\,dy\,K(x,y)P_{2n-l_p-1}(x)P_{2m-l_p-1}(y) = \sum_{\alpha,\beta=1}^{N-l_p} w_\alpha w_\beta K(x_\alpha,y_\beta)P_{2n-l_p-1}(x_\alpha)P_{2m-l_p-1}(y_\beta). \tag{12}$$

The required number N of polynomials is determined by the convergence of the expansion $xj_l(x)\simeq\Sigma_{n=1}^{N}j_{ln}P_{2n-l_p-1}(x)$ in the interval $0\leqslant x\leqslant\kappa$. Figure 1 shows the number of polynomials N required to obtain a given error in the expansion, as a function of κ, for $l=0$. The l dependence of the error is very small and, as a rule of thumb, we use $N=\mathrm{int}(10+0.65\kappa)$.

Figure 2 plots the first eigenfunctions $\phi_i(x)$ of the filter kernel $K^2(x,y)$ for a typical value of κ, and Fig. 3 shows all the eigenvalues λ_i^2 up to N. It may be seen that there is a rapid transition between the eigenvalues which are very close to 1 and those close to 0. It is then straightforward to select the M eigenfunctions whose eigenvalues are above some threshold, say $\lambda_i^2>0.99$, for the expansion of the filtered function:

$$f(x) \leftarrow \sum_{i=1}^{M} f_i\phi_i(x), \tag{13}$$

$$f_i = \sum_{\alpha=1}^{N-l_p} w_\alpha\phi_i(x_\alpha)f(x_\alpha). \tag{14}$$

Figure 4 shows, as an example, the unfiltered and filtered oxygen $2p$ pseudo-atomic-orbital, generated as proposed by Sankey and Niklewski[6,10] with a Troullier-Martins pseudopotential.[11] To enhance the filtering effect, we have used a very small filter cutoff. Still, it may be seen that the Fourier components above the cutoff are very efficiently suppressed, although this is achieved (with this small cutoff) at the expense of a substantial change in its shape.

Finally, the most confined eigenfunctions $\phi_1(x)$ for each angular momentum l may be used to generate a localized

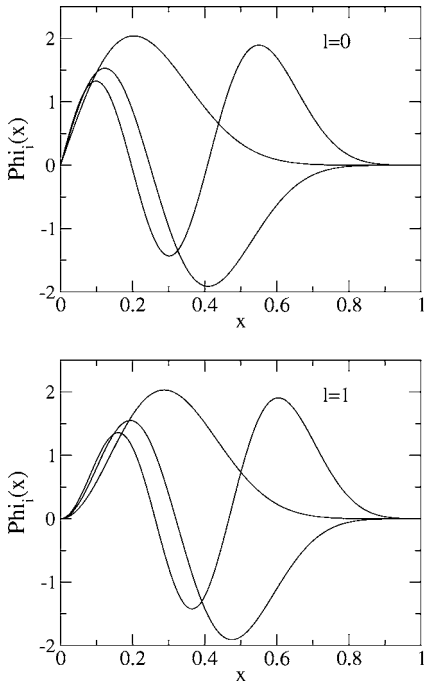

FIG. 2. First few eigenfunctions (with highest eigenvalues) of the filter kernel $K^2(x,x')$ for $\kappa \equiv k_c r_c = 25$. Divided by r, they give the radial part of the distributions, with angular momentum l, that are most localized in a real-space sphere of radius r_c and simultaneously in a reciprocal-space sphere of radius k_c.

distribution with given multipole moments, as required in the ultrasoft pseudopotential[5] and projector augmented wave[12] methods, among other problems in computational physics.[2] They may be used also as a basis of localized orbitals, for the expansion of the electron wavefunctions,[13] which is asymptotically complete, within the confining spheres, as the filter cutoff increases.

III. APPLICATION WITHIN SIESTA

There are three contributions to the eggbox effect in SIESTA (an artificial rippling of the total energy surface as a function of the positions of the atoms relative to the integration grid points). (i) First is the so-called neutral-atom potential[6] $V_{NA}(\mathbf{r})$ given by the local part of the atomic pseudopotentials minus the Hartree potential of the free-atom

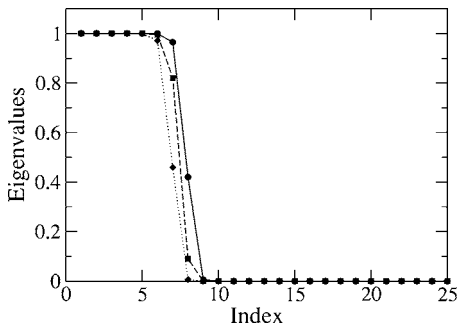

FIG. 3. Eigenvalues of the filter kernel $K^2(x,x')$ for $\kappa=25$ and $l=0$ (circles and full line), 1 (squares and dashed line), and 2 (diamonds and dotted line).

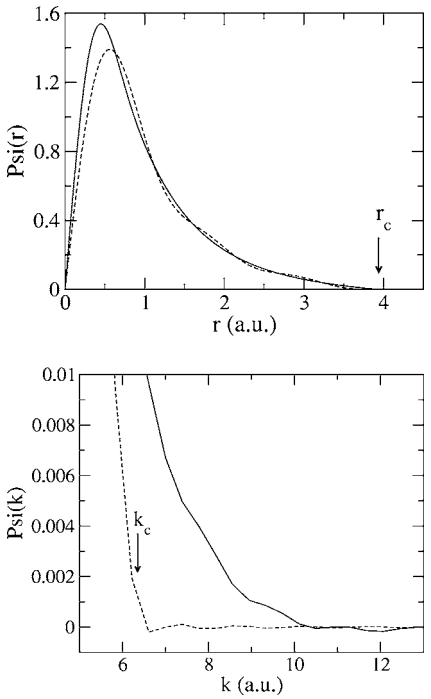

FIG. 4. Filtered (dashed lines) and unfiltered (full lines) oxygen $2p$ pseudo-atomic-orbital, generated with a strict cutoff $r_c = 3.94$ bohr as proposed by Sankey and Niklewski (Ref. 10). It was filtered with a cutoff $\kappa=25$, which corresponds to a plane-wave cutoff $k_c = 6.35$ bohr^{-1}, or $k_c^2 = 40$ Ry. Upper panel: real-space shape. Lower panel: tails of their Fourier transforms.

electron densities. (ii) Second is the exchange and correlation potential $V_{xc}(\mathbf{r})$, given by the electron valence density $\rho(\mathbf{r})$, which in turn is given by a sum of products of atomic basis orbitals $\varphi_\mu(\mathbf{r})$. These two contributions are frequently comparable in magnitude. (iii) There is also the nonlocal core correction (NLCC) to $V_{xc}(\mathbf{r})$, given by a pseudocore electron density $\rho_{NLCC}(\mathbf{r})$ added to $\rho(\mathbf{r})$. This added density is generally very large and localized and, when the NLCC is present, it normally dominates the eggbox effect. Finally, the Hartree energy, given by the self-interaction of $\rho(\mathbf{r})$, also contributes to the eggbox but, since the Hartree potential is much smoother than the density, this contribution is always negligible compared to the other ones.

Thus, in order to cut drastically the eggbox effect, we must filter $\rho_{NLCC}(\mathbf{r})$, $V_{NA}(\mathbf{r})$, and $\varphi_\mu(\mathbf{r})$. The first two may be filtered with the plane-wave cutoff k_c of the real-space integration grid used to calculate the matrix elements of $V_{NA}(\mathbf{r})$ and $V_{xc}(\mathbf{r})$. The filtering cutoff required for $\varphi_\mu(\mathbf{r})$ is somewhat less clear, because we need to treat products of two φ's in the integration grid, not just the φ's themselves. In principle, the plane-wave cutoff of a product of two functions is twice that of the functions themselves, which would suggest that $\varphi_\mu(\mathbf{r})$ should be filtered with $k_c/2$. However, a widespread experience with plane-wave codes has shown that this criterion is too strict, and that in practice the effective cutoff for the density is typically less than two times that of the wave functions. Therefore, we have checked that making the filter cutoff for $\varphi_\mu(\mathbf{r})$ equal to $\sim 0.6 k_c$ leads generally to the best convergence, as a function of k_c.

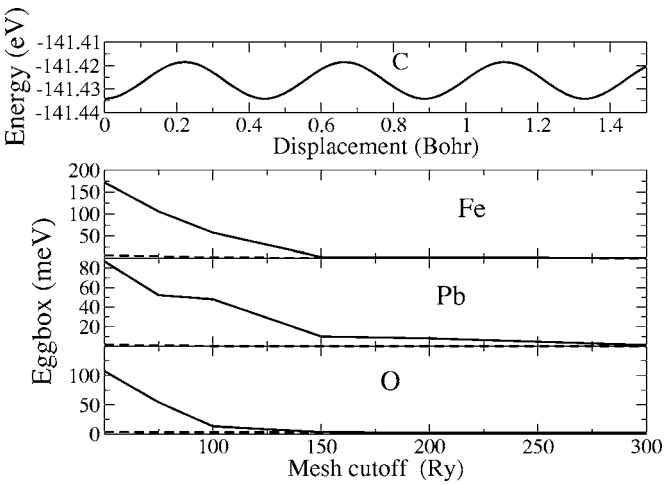

FIG. 5. (a) Total energy of an isolated carbon atom, as it is displaced in a large unit cell, using an integration grid with a plane-wave cutoff $k_c^2=50$ Ry, whose points are separated by $\Delta x=\pi/k_c=0.44$ bohr. (b) Magnitude of the eggbox effect (peak to peak of total energy) for several isolated atoms with hard pseudopotentials or nonlocal core corrections (in Pb and Fe), as a function of the plane-wave cutoff of the integration mesh. Full lines, without filtering; dashed lines, with filtering.

Figure 5 shows the eggbox effect of isolated atoms displaced across the integration mesh. It may be seen that the effect is indeed eliminated almost completely by filtering. Of course, we shall not eliminate the eggbox effect at the expense of filtering the pseudopotentials and basis functions so much as to change the physical results. Figure 6 shows the vibrational frequencies of the water molecule, calculated by diagonalizing the dynamical matrix obtained by finite differences.[14] As the plane-wave cutoff k_c of the integration grid is reduced, $\rho_{NLCC}(\mathbf{r})$ and $V_{NA}(\mathbf{r})$ are filtered with that cutoff, and $\varphi_\mu(\mathbf{r})$ is filtered with $0.7k_c$. It may be seen that much lower cutoffs are required, to converge accurate frequencies, with than without filtering.

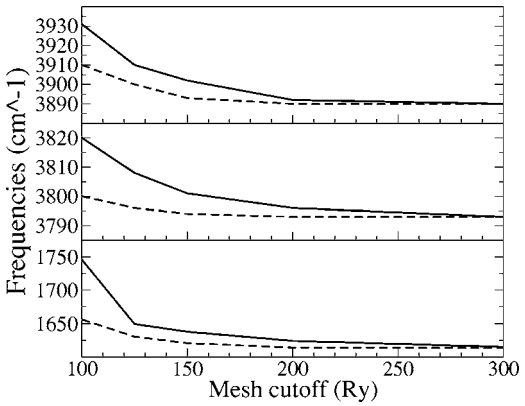

FIG. 6. Vibrational frequencies of the water molecule, calculated from the Hessian matrix, which was obtained by finite differences from the forces on the atoms displaced from their equilibrium positions. The x axis is the plane wave cutoff of the integration grid used in SIESTA. Full lines, without filtering; dashed lines, with filtering.

IV. CONCLUSIONS

We have presented a general method to generate distributions, with a given angular momentum, which are optimally confined within a strict cutoff in both real and Fourier space. They can be used by themselves, as to produce localized distributions with given multipole moments, or as a basis for expanding and filtering an arbitrary initial distribution. As an example, we have shown how they can be used to filter the pseudopotentials and basis functions in the density functional method SIESTA, thus eliminating the eggbox effect on the total energy, due to the calculation of matrix elements in a real space integration grid.

ACKNOWLEDGMENTS

We want to thank Alberto García for useful discussions and M. Fernández-Serra for the basis set of the water molecule.[15] This work has been funded by Grant No. BFM2003-03372 from the Spanish Ministery of Science.

APPENDIX: VARIATIONAL PRINCIPLES

Here we show that the filtering basis functions $\phi_i(r)$ obey a simple variational principle, and we also present an alternative principle for Gaussian basis functions. It may be easily shown, by a straightforward functional derivative, that the eigenvalue equation (7) is equivalent to the variational principle

$$\int_0^1 \int_0^1 dx\, dx'\, \phi(x) K^2(x,x') \phi(x') = \max, \tag{A1}$$

subject to the condition of normalization of $\phi(x)$ within $0 \leqslant x \leqslant 1$. Now, using that the Fourier transform of $\phi(x)$ is

$$g(y) = \int_0^1 dx\, \phi(x) K(x,y) \tag{A2}$$

as well as the definition (6) and the fact that the total norm of a function is the same in real and Fourier space:

$$\int_0^1 dy \int_0^1 dx\, \phi(x) K(x,y) \int_0^1 dx' K(y,x') \phi(x') = \int_0^1 dy\, g^2(y)$$
$$= 1 - \int_1^\infty dy\, g^2(y) = \max \Rightarrow \int_1^\infty dy\, g^2(y) = \min. \tag{A3}$$

Thus, our basis functions $\phi(x)$ are the normalized distributions which are strictly confined to $0 \leqslant x \leqslant 1$ (i.e., $r \leqslant r_c$) and whose Fourier transform has the smallest norm in $y > 1$ ($k > k_c$).

Interestingly, an alternative variational principle may be demonstrated for a basis of gaussian functions. Thus, we

maximize the confinement of a normalized distribution $\phi(\mathbf{r})$ and its Fourier transform $\phi(\mathbf{k})$, in the sense of least squared dispersion:

$$\frac{1}{r_c^2}\int d\mathbf{r}\,\mathbf{r}^2\phi^2(\mathbf{r}) + \frac{1}{k_c^2}\int d\mathbf{k}\,\mathbf{k}^2\phi^2(\mathbf{k}) = \min \qquad \text{(A4)}$$

where r_c and k_c are here scale factors that determine the relative confinement in real and Fourier space, rather than strict cutoffs. Multiplying by $k_c^2/2$:

$$\int d\mathbf{r}\frac{k_c^2\mathbf{r}^2}{2r_c^2}\phi^2(\mathbf{r}) + \int d\mathbf{k}\frac{\mathbf{k}^2}{2}\phi^2(\mathbf{k}) = \min. \qquad \text{(A5)}$$

Now, the first term is the potential energy of a quantum harmonic oscillator with spring constant $(k_c/r_c)^2$ and wave function $\phi(\mathbf{r})$, and the second term is its kinetic energy. Its well-known solutions are Gaussians times Hermite polynomials.[16] A similar (but not orthonormal) basis, made of Gaussians times powers of r, was used by Hartwigsen *et al.*[17] to generate compact separable pseudopotentials.

[1] W. H. Press, S. A. Teukolsky, W. T. Vetterling, and B. P. Flannery, *Numerical Recipes* (Cambridge University Press, Cambridge, U.K., 1992).

[2] R. W. Hockney and J. W. Eastwood, *Computer Simulation Using Particles* (IOP Publishing, Bristol, 1988).

[3] R. D. King-Smith, M. C. Payne, and J. S. Lin, Phys. Rev. B **44**, 13063 (1991).

[4] L. Kleinman and D. M. Bylander, Phys. Rev. Lett. **48**, 1425 (1982).

[5] D. Vanderbilt, Phys. Rev. B **41**, R7892 (1990).

[6] J. M. Soler, E. Artacho, J. D. Gale, A. García, J. Junquera, P. Ordejón, and D. Sánchez-Portal, J. Phys.: Condens. Matter **14**, 2745 (2002).

[7] P. Ordejón, E. Artacho, and J. M. Soler, Phys. Rev. B **53**, R10441 (1996).

[8] T. L. Beck, Rev. Mod. Phys. **72**, 1041 (2000).

[9] E. L. Briggs, D. J. Sullivan, and J. Bernholc, Phys. Rev. B **54**, 14362 (1996).

[10] O. F. Sankey and D. J. Niklewski, Phys. Rev. B **40**, 3979 (1989).

[11] N. Troullier and J. L. Martins, Phys. Rev. B **43**, 1993 (1991).

[12] P. E. Blöchl, Phys. Rev. B **50**, 17953 (1994).

[13] C. K. Gan, P. D. Haynes, and M. C. Payne, Phys. Rev. B **63**, 205109 (2001).

[14] To obtain the full Hessian matrix by finite differences, M. Paulsson has noticed that the eggbox effect can be dramatically reduced by using not the force on the displaced atom but minus the total force on the rest of the atoms (for details, http://www.uam.es/siesta). This trick cannot be used, however, when many atoms move simultaneously, as to calculate given frozen-phonon frequencies or in molecular dynamics. Therefore, we have used the forces of the displaced atoms to obtain the Hessian, precisely to evaluate the effect of filtering on the eggbox.

[15] M. Fernandez-Serra and E. Artacho, J. Chem. Phys. **121**, 11136 (2004).

[16] C. Cohen-Tannoudji, B. Diu, and F. Laloë, *Mécanique Quantique* (Hermann, Paris, 1977).

[17] C. Hartwigsen, S. Goedecker, and J. Hutter, Phys. Rev. B **58**, 3641 (1998).